

# Automated, Quantitative Screening Assay for Antiangiogenic Compounds Using Transgenic Zebrafish

T. Cameron Tran,<sup>1</sup> Blossom Sneed,<sup>2</sup> Jamil Haider,<sup>1</sup> Delali Blavo,<sup>1</sup> Audrey White,<sup>1</sup> Temitope Aiyejorun,<sup>1</sup> Timothy C. Baranowski,<sup>1</sup> Amy L. Rubinstein,<sup>1</sup> Thanh N. Doan,<sup>1</sup> Raymond Dingleline,<sup>2</sup> and Eric M. Sandberg<sup>1</sup>

<sup>1</sup>Zygon, LLC, and <sup>2</sup>Chemical Biology Discovery Center and Department of Pharmacology, Emory University, Atlanta, Georgia

## Abstract

**Pathologic angiogenesis has emerged as an important therapeutic target in several major diseases. Zebrafish offer the potential for high-throughput drug discovery in a whole vertebrate system. We developed the first quantitative, automated assay for antiangiogenic compound identification using zebrafish embryos. This assay uses transgenic zebrafish with fluorescent blood vessels to facilitate image analysis. We developed methods for automated drugging and imaging of zebrafish in 384-well plates and developed a custom algorithm to quantify the number of angiogenic blood vessels in zebrafish. The assay was used to screen the LOPAC1280 compound library for antiangiogenic compounds. Two known antiangiogenic compounds, SU4312 and AG1478, were identified as hits. Additionally, one compound with no previously known antiangiogenic activity, indirubin-3'-monoxime (IRO), was identified. We showed that each of the hit compounds had dose-dependent antiangiogenic activity in zebrafish. The IC<sub>50</sub> of SU4312, AG1478, and IRO in the zebrafish angiogenesis assay was 1.8, 8.5, and 0.31 μmol/L, respectively. IRO had the highest potency of the hit compounds. Moreover, IRO inhibited human umbilical vein endothelial cell tube formation and proliferation (IC<sub>50</sub> of 6.5 and 0.36 μmol/L, respectively). It is therefore the first antiangiogenic compound discovered initially in a zebrafish assay that also has demonstrable activity in human endothelial cell-based angiogenesis assays. [Cancer Res 2007;67(23):11386–92]**

## Introduction

Angiogenesis is a well-established therapeutic target. Several angiogenesis assays are currently used for drug screening (1). Endothelial cell models of migration, proliferation, apoptosis, and tube formation are popular due to their simplicity and throughput. However, these assays lack the biological complexity of *in vivo* systems. Animal models, including the chick chorioallantoic membrane assay, corneal neovascularization assay, and Matrigel plug assay preserve biological complexity but are costly and low throughput. Zebrafish provide a system for drug screening that combines the biological complexity of *in vivo* models with the

ability for much higher-throughput screening than other available animal models.

Blood flow begins in the zebrafish embryo at ~24 h postfertilization. Shortly after this, the angiogenic vessels that perfuse the trunk of the embryo (intersegmental vessels) sprout from the vasculogenic vessels (2). Major molecular pathways regulating angiogenesis in mammalian systems are conserved in zebrafish (3, 4). Studies have shown that treatment of zebrafish embryos with clinical stage antiangiogenic compounds inhibits growth of angiogenic blood vessels, suggesting that larger-scale antiangiogenic compound screening in zebrafish is possible (5–7).

We developed an automated, quantitative screening assay for the discovery of antiangiogenic compounds using zebrafish. Transgenic zebrafish expressing green reef coral fluorescent protein (GRCFP) under the control of the vascular endothelial growth factor receptor (VEGFR) 2 promoter [*TG(VEGFR2:GRCFP)*] for blood vessel-restricted expression were used for this assay. The creation of this line was described previously (6). The assay includes automated methods for compound delivery and embryo imaging in 384-well plates. Additionally, we developed a custom algorithm for quantifying the growth of angiogenic vessels in zebrafish embryos. Using this assay, we screened the LOPAC1280 compound library for antiangiogenic activity and identified three hit compounds. The most potent, indirubin-3'-monoxime (IRO), has not been previously reported to have antiangiogenic activity. Furthermore, IRO inhibits human endothelial cell tube formation and proliferation, and is therefore the first antiangiogenic compound discovered in zebrafish whose activity subsequently translated to human cell-based assays.

## Materials and Methods

**Zebrafish husbandry.** Adult zebrafish were maintained at 27°C in a recirculating aquaculture system (8). Fertilized eggs were obtained from adult mating pairs, treated with Pronase to remove chorions, and raised in Holtfreter's solution (60 mmol/L NaCl, 2.4 mmol/L sodium bicarbonate, 0.8 mmol/L CaCl<sub>2</sub>, 0.67 mmol/L KCl, and 10 mmol/L HEPES) in a humidified incubator at 27°C.

**Library screening (primary screen).** The LOPAC1280 library was obtained from Sigma. *TG(VEGFR2:GRCFP)* embryos were arrayed into 384-well plates (one embryo per well) in 30 μL of Holtfreter's solution at 1 day postfertilization. The positive control for this assay was 10 μmol/L PTK787, a VEGFR antagonist, and the negative control was 1% DMSO. Automated drugging was performed using a Sciclone ALH3000 robotic liquid handler (Caliper Life Sciences). A 60-μmol/L working stock of each compound was prepared in Holtfreter's solution, and 30 μL of the working stock was added to each well of the 384-well plate, resulting in a final screening concentration of 30 μmol/L. Five embryos per compound were dosed. At 2 days postfertilization, zebrafish were anesthetized with 0.016% tricaine and a fluorescent image of each embryo was captured automatically using the Discovery-1 or ImageXpress imaging systems (Molecular Devices). Images of zebrafish embryos were captured using a Nikon CFI PlanApo 2×

**Note:** Supplementary data for this article are available at Cancer Research Online (<http://cancerres.aacrjournals.org/>).

T.C. Tran and B. Sneed contributed equally to this work.

**Requests for reprints:** Eric Sandberg or Amy Rubinstein, Zygon, LLC, 24 Peachtree Center Avenue, 520 Kell Hall, Atlanta, GA 30303. Phone: 404-523-7309; E-mail: [eric@zygon.com](mailto:eric@zygon.com) or [amy@zygon.com](mailto:amy@zygon.com).

©2007 American Association for Cancer Research.

doi:10.1158/0008-5472.CAN-07-3126

objective (numerical aperture, 0.10; working distance, 8.5 mm; focal length, 100 mm); camera exposure, 75 ms; camera binning, 2; gain, 2; with a FITC fluorescence filter set and autofocus in each well. Trunks of the zebrafish were isolated from fluorescent images using MetaMorph software, and a custom automated algorithm (described below) was used to count intersegmental vessels and their branching arteries. Because the trunk isolation step of the journal was interactive, each image was viewed by the user during the analysis, allowing exclusion of images showing embryos that were unhealthy or in an improper orientation for analysis. Percent control was defined as  $100 \times (C - \text{PTK787}) / (\text{DMSO} - \text{PTK787})$ , where  $C$ , PTK787, and DMSO represent the mean vessel count in the presence of compound, PTK787, and DMSO, respectively. A 384-well plate required ~30 min for image acquisition and ~20 min for data analysis.

Experimental log  $P$  values for compounds were obtained from DrugBank<sup>3</sup> or ChemIDPlus Advanced.<sup>4</sup>

**Design of the automated algorithm for quantifying angiogenesis in zebrafish.** An interactive algorithm (journal) was developed using the Discovery-1/MetaMorph software to rapidly analyze each image. The key component of the analysis was counting the number of intersegmental vessels and branching arteries in the isolated trunk of the embryo using the MetaMorph Neurite Outgrowth application drop-in. The application settings identified the vasculogenic vessels as one or more cell bodies and the angiogenic vessels as outgrowths of these cell bodies. Vasculogenic vessels (cell bodies) were differentiated from their branching arteries (outgrowths) by their larger width and greater fluorescence intensity. The application settings for identification of cell bodies were as follows: approximate maximum width, 160  $\mu\text{m}$ ; intensity above local background, 120 gray levels; and minimum area, 2,000  $\mu\text{m}^2$ . The application settings for identification of outgrowths were as follows: maximum width is 33  $\mu\text{m}$  and intensity above local background is 45 gray levels. The data (number of intersegmental vessels and branching arteries) were exported as a summary log to Microsoft Excel.

**Secondary screens.** Follow-up studies, including dose-response studies, were performed using zebrafish expressing AcGFP under the control of the VEGFR2 promoter, [TG(VEGFR2:AcGFP)]. This line responds similarly to the TG(VEGFR2:GRCFP) line when treated with antiangiogenic compounds (data not shown). Zebrafish were anesthetized and mounted in methyl cellulose for imaging. Images were acquired using a Leica MZ16FA fluorescent microscope equipped with an AxioCam MRc5 camera.

**Human umbilical vascular endothelial cell assays.** Human umbilical vascular endothelial cell (HUVEC) assays were performed by Southern Research Institute. HUVECs and medium were purchased from Lonza Group Ltd. For all HUVEC assays, cells were grown in a 37°C incubator under 5% CO<sub>2</sub>. Full-growth medium for HUVECs was endothelial cell basal medium (EBM) supplemented with 2% fetal bovine serum, 12  $\mu\text{g}/\text{mL}$  bovine brain extract, 1  $\mu\text{g}/\text{mL}$  hydrocortisone, and 1  $\mu\text{g}/\text{mL}$  GA-1000 (gentamicin-amphotericin). HUVECs were used between passages 3 and 12.

**[<sup>3</sup>H]thymidine incorporation assay.** HUVECs were seeded into 96-well plates (6,250 cells per well) in growth medium. After 24 h, various doses of IRO were added to the cultures. After 3 days of treatment, the HUVEC cultures were pulsed with 1  $\mu\text{Ci}$  of [<sup>3</sup>H]thymidine for 8 h and harvested with a semiautomatic cell harvester onto DNA-binding filters. The filters were counted in a Perkin-Elmer Microbeta scintillation counter (Trilux) to determine the amount of [<sup>3</sup>H]thymidine incorporation.

**CellTiter-Glo luminescent cell viability assay.** The CellTiter-Glo luminescent cell viability assay quantifies total ATP levels in cells, which reflects the relative number of viable cells. The assay was performed according to the manufacturer (Promega). Briefly, HUVECs were seeded into 96-well plates (6,250 cells per well) in growth medium. After 24 h, IRO was added to the cultures at the indicated concentrations. After 3 days of treatment, CellTiter-Glo reagent was added to the cultures and luminescent signal was measured with an EnVision Multilabel Reader (Perkin-Elmer). Controls were treated with vehicle (DMSO).

**HUVEC tube formation.** The *in vitro* angiogenesis assay kit (Millipore) was used for tube formation studies. HUVECs were seeded into 96-well plates (15,000 cells per well) coated with ECMatrix (Millipore), consisting of laminin, collagen type IV, heparin sulfate proteoglycans, entactin, and nidogen. The cells were treated with IRO at the indicated concentrations. Controls were treated with vehicle (DMSO). The cells were allowed to form endothelial tubes for 18 h and then examined under an inverted light microscope. Microscopic fields were photographed and quantitatively analyzed using Image Pro Plus software, which detects tubule extensions from endothelial cell bodies, to determine tubule length. Tubule length was measured as an average of three fields of view in each well.

**HUVEC migration.** The transwell migration chamber of the biocoat endothelial cell migration angiogenesis system (BD Bioscience) was used for endothelial cell migration assays. Chamber inserts were equilibrated at 37°C in EBM containing 0.1% bovine serum albumin (BSA) for 1 h. Endothelial cells were starved for 4 to 5 h in EBM containing 0.1% BSA before harvesting. The endothelial cells were then seeded into the upper chambers of the transwell system ( $1 \times 10^5$  cells per well) in 100  $\mu\text{L}$  of EBM containing 0.1% BSA and IRO at the indicated concentrations. Full growth medium was added to the bottom chamber as a chemoattractant. Cell migration through the filter was allowed to proceed for 22 h. Unmigrated cells on the top of the filters were removed, and migrated cells on the bottom of the filters were fixed with 4% paraformaldehyde and stained with Hoechst 33342. Three microscopic fields for each filter were used to count the number of migrated cells and determine an average for that filter.

**Statistical methods.** The screening  $Z'$  factor, signal-to-background (S:B) ratio, and signal-to-noise (S:N) ratio for the zebrafish screening assay were calculated by averaging the values for each plate analyzed.  $Z'$  factor =  $1 - [3 \times (\sigma_p + \sigma_n) / |\mu_p - \mu_n|]$ , where  $\mu_p$  and  $\sigma_p$  are the mean and SD of the positive control (PTK787) and  $\mu_n$  and  $\sigma_n$  are mean and SD for the negative control (9). S:B =  $\mu_p/\mu_n$  and S:N =  $(\mu_p - \mu_n)/\text{sqrt}(\sigma_p^2 + \sigma_n^2)$ . Statistical significance for experiments was determined using unpaired Student's  $t$  tests and  $P < 0.05$ .

## Results

**Screening for antiangiogenic compounds using live zebrafish.** TG(VEGFR2:GRCFP) zebrafish embryos with fluorescent blood vessels were used to screen the LOPAC1280 compound library for antiangiogenic activity. Screening was performed collaboratively between Zygogen and Emory University. Half of the library (640 compounds) was screened at each site. Adult mating pairs were set up in the evening, and fertilized eggs were collected the next morning. Embryos were drugged one day after fertilization in the morning, before formation of the angiogenic intersegmental vessels. For drugging, zebrafish were manually arrayed into 384-well plates (one embryo per well; five embryos per condition) using a 200- $\mu\text{L}$  wide-bore pipette tip (to avoid damaging the embryos) and treated with 30  $\mu\text{mol}/\text{L}$  of each test compound using a robotic liquid handling instrument. Before arraying the plate, unhealthy or developmentally delayed embryos were removed by examination under a bright field microscope. All plates contained both negative controls (1% DMSO) and positive controls [10  $\mu\text{mol}/\text{L}$  PTK787, a VEGFR antagonist that potently inhibits angiogenic blood vessel growth in the head and trunk of zebrafish (ref. 5; Fig. 1A)]. After overnight incubation with test compounds, a fluorescent image of each zebrafish embryo in the 384-well plate was captured using an automated imaging system. The trunk of each zebrafish in the fluorescent image was isolated using MetaMorph software. An automated custom algorithm was used to quantify the number of angiogenic vessels in the zebrafish trunk (Fig. 1B). A detailed description of this algorithm is included in Materials and Methods.

Hits were defined as compounds that caused an inhibition of angiogenic vessel growth that was three times greater than the SD

<sup>3</sup> <http://redpoll.pharmacy.ualberta.ca/drugbank/>

<sup>4</sup> <http://chem.sis.nlm.nih.gov/chemidplus/>

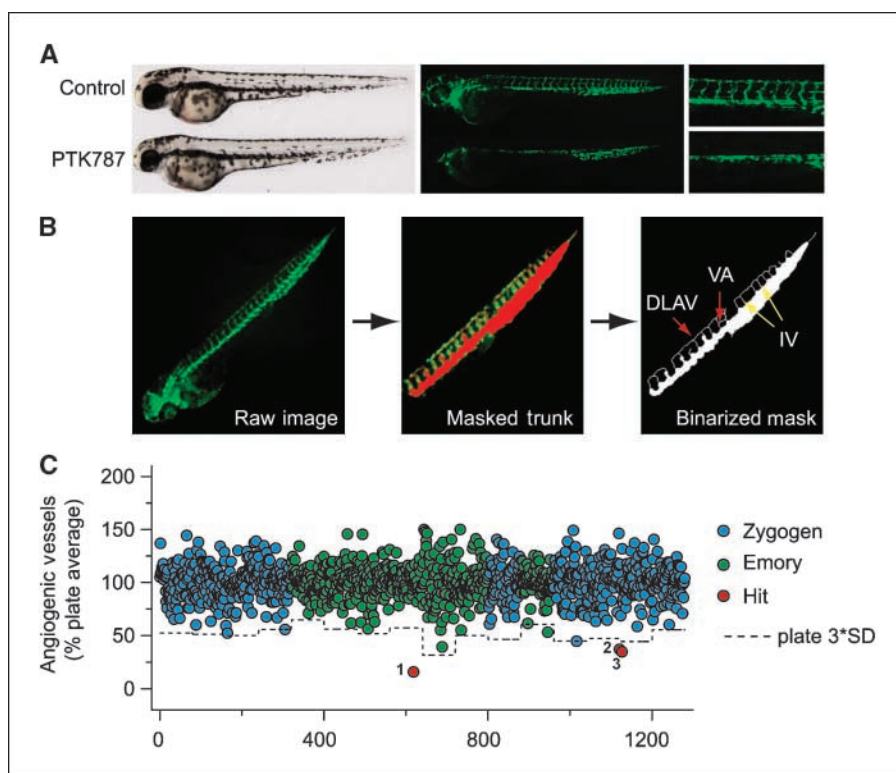


**Figure 1.** The LOPAC1280 library was screened for antiangiogenic compounds using transgenic zebrafish. *A*, bright field and fluorescent images of 2-d postfertilization zebrafish treated overnight with 1% DMSO (*control*; vehicle control for the assay) and 10  $\mu\text{mol/L}$  PTK787 (positive control for the assay). Angiogenic blood vessel growth is inhibited in the head and trunk of the PTK787-treated embryos. *B*, for quantification of angiogenic vessel growth in zebrafish embryos, the trunk is manually isolated from the fluorescent image. An automated algorithm masks the vasculogenic vessels based on fluorescence signature and size (*masked trunk*), and a binarized image is created from the masked image (*binarized mask*). The intersegmental vessels (*IV*) and their branching arteries, the vertebral artery (*VA*) and dorsal longitudinal anastomatic vessel (*DLAV*), are counted by the software. *C*, the LOPAC1280 library was screened jointly by Zygogen (*blue points*) and Emory University (*green points*). *Points*, mean value of up to five embryos tested for each compound. Data were normalized as percentage of plate average (average vessel count of all test compounds on plate). Positive hits (*red points*) were defined as compounds that caused an inhibition of angiogenic vessel count  $>3$  SDs from the plate average. IRO, 1; SU4312, 2; AG1478, 3.

for compound responses in each plate (Fig. 1C). Forty compounds, representing 3.1% of the total library, were severely toxic or lethal at the screening dose and were not analyzed further. The screen had robust quality control measures, with mean plate  $Z'$  factor of 0.58, S:B of 4.8, and S:N of 10.2.

Three hits were identified in the screen, representing a 0.23% hit rate. Two of these compounds, SU4312 (a VEGFR and platelet-derived growth factor receptor antagonist), and AG1478 (an epidermal growth factor receptor antagonist), are known to have antiangiogenic activity (10, 11), although this is the first report showing antiangiogenic activity of these compounds in zebrafish. The other hit compound, IRO, has not been previously described as antiangiogenic. Inhibition of angiogenesis by IRO was confirmed with freshly purchased compound from another source (VWR). In subsequent experiments, 24-h postfertilization zebrafish embryos were treated with each of the hit compounds for 4 or 24 h. All three compounds showed antiangiogenic activity at both time points (Figs. 2A and B, 3A and B, and 4A and B). Additionally, each of the three compounds caused a dose-dependent inhibition of angiogenic vessel growth in 2-day postfertilization zebrafish that had been treated overnight (Fig. 2C, Fig. 3C, and Fig. 4C), with IRO having the highest potency ( $\text{IC}_{50}$ , 0.31  $\mu\text{mol/L}$ ). The  $\text{IC}_{50}$  for SU4312 and AG1478 was 1.8  $\mu\text{mol/L}$  and 8.5  $\mu\text{mol/L}$ , respectively.

Five compounds [SU5416, 2-methoxyestradiol, difluoromethylornithine (DFMO) hydrochloride, minocycline hydrochloride, and thalidomide] in the LOPAC1280 library that are listed as antiangiogenic in the compound description were not scored as hits during the screen. The reasons why these compounds were negative in the assay are as follows: SU5416 was lethal at the 30- $\mu\text{mol/L}$  screening dose but was antiangiogenic in zebrafish at sublethal doses (6). 2-Methoxyestradiol was also toxic at the screening dose, but the embryos survived, showing

severely bent trunks and cardiac edema. 2-Methoxyestradiol reduced intersegmental vessel growth, but it was unclear if these effects were a result of toxicity. We found that 2-methoxyestradiol was antiangiogenic when tested at a lower dose (10  $\mu\text{mol/L}$ ), and that the toxicity was reduced (data not shown). The antiangiogenic effects of 2-methoxyestradiol in zebrafish are consistent with previously published work (7). It is likely that the three other compounds (DFMO hydrochloride, minocycline hydrochloride, and thalidomide) failed to inhibit angiogenesis in the zebrafish because they are highly hydrophilic, with  $\log P$  values less than 1 ( $-0.49$  for DFMO, 0.092 for minocycline, and  $-0.146$  for thalidomide). Compounds with  $\log P$  values less than 1 are typically not well-absorbed from the medium by zebrafish embryos (12).<sup>5</sup>

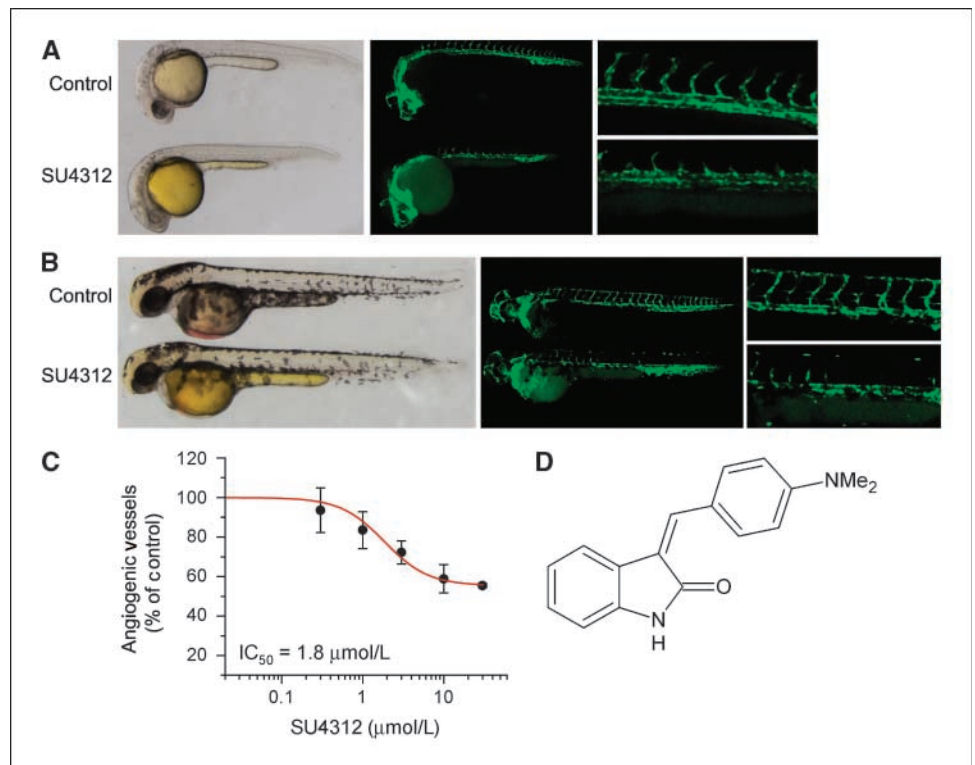
**IRO does not affect vasculogenic vessel development or preexisting vasculature.** Because the intersegmental vessels in zebrafish form by sprouting from the preformed vasculogenic vessels, any compound that disrupts vasculogenesis will also inhibit the growth of angiogenic vessels. To determine the effect of IRO on vasculogenesis, zebrafish embryos were treated with 1  $\mu\text{mol/L}$  IRO at 10 h postfertilization. This time point precedes the appearance of angioblasts, which differentiate to form the vasculogenic vessels. Treatment of zebrafish at this early time point had a very strong antiangiogenic effect, causing nearly complete inhibition of intersegmental vessel growth. The vasculogenic dorsal aorta and posterior cardinal vein were unaffected (Supplementary Fig. S1).

To determine if IRO has an effect on established vasculature, zebrafish embryos were treated with IRO beginning at 3 days postfertilization, an age when intersegmental vessels have formed completely and are stabilized. Embryos were imaged at

<sup>5</sup> Zygogen, unpublished data.



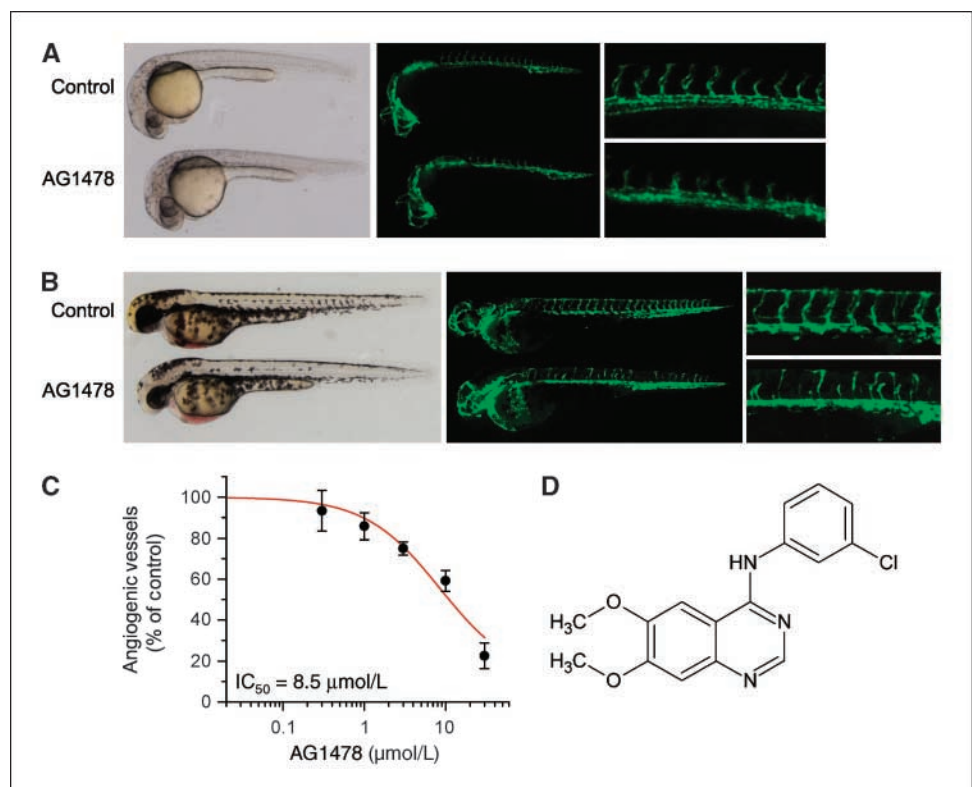
**Figure 2.** SU4312 inhibits angiogenic vessel growth in zebrafish embryos. **A**, bright field and fluorescent images of 28-h postfertilization zebrafish treated for 4 h with 1% DMSO (*control*) or 30  $\mu\text{mol/L}$  SU4312 and 2-d postfertilization zebrafish treated overnight with 1% DMSO (*control*) or 30  $\mu\text{mol/L}$  SU4312 (**B**). **C**, SU4312-mediated antiangiogenic effects are dose dependent. **D**, structure of SU4312. *Points*, mean for three independent dose-response experiments ( $n = 19\text{--}30$  total embryos for each condition); *bars*, SE.



4 days postfertilization (Supplementary Fig. S2A), and the number of angiogenic vessels in the trunk was quantified (Supplementary Fig. S2B). IRO had no effect on the preexisting vessels, demonstrating that its effects are cytostatic, not

cytotoxic. Taken together, the data in Supplementary Figs. S1 and S2 show that IRO has specific antiangiogenic activity because it does not affect vasculogenesis and does not target established blood vessels.

**Figure 3.** AG1478 inhibits angiogenic vessel growth in zebrafish embryos. **A**, bright field and fluorescent images of 28-h postfertilization zebrafish treated for 4 h with 1% DMSO (*control*) or 30  $\mu\text{mol/L}$  AG1478 and 2-d postfertilization zebrafish treated overnight with 1% DMSO (*control*) or 10  $\mu\text{mol/L}$  AG1478 (**B**). AG1478 inhibits angiogenic vessel growth in the trunk of zebrafish embryos. **C**, AG1478-mediated antiangiogenic effects are dose dependent. **D**, structure of AG1478. *Points*, mean of three independent dose-response experiments ( $n = 15\text{--}29$  total embryos for each condition); *bars*, SE.



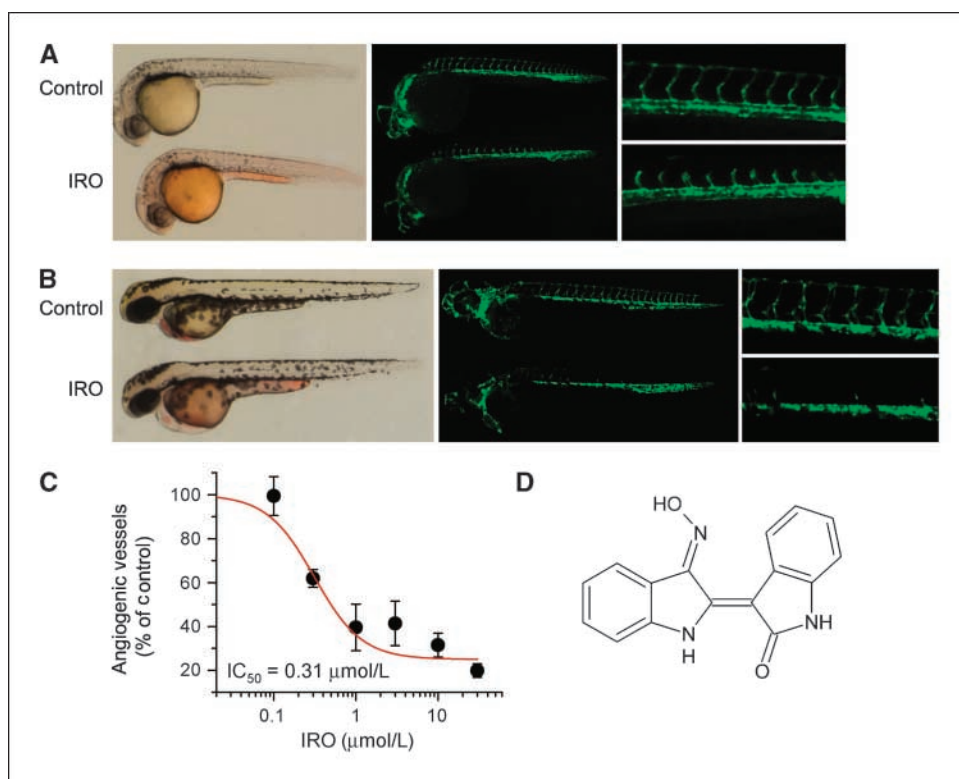


**Figure 4.** IRO inhibits angiogenic vessel growth in zebrafish embryos. *A*, bright field and fluorescent images of 28-h postfertilization zebrafish treated for 4 h with 1% DMSO (*control*) or 30  $\mu\text{mol/L}$  IRO and 2-d postfertilization zebrafish treated overnight with 1% DMSO (*control*) or 10  $\mu\text{mol/L}$  IRO (*B*). IRO inhibits angiogenic vessel growth in the trunk of zebrafish embryos. *C*, IRO-mediated antiangiogenic effects are dose dependent. *D*, structure of IRO. Points, mean of three independent dose-response experiments ( $n = 24\text{--}35$  total embryos for each condition); bars, SE.

**Antiangiogenic activity of IRO in human endothelial cell assays.** To determine if IRO is antiangiogenic in human endothelial cells and to elucidate its mechanism of action on endothelium, IRO was assessed in human umbilical cord vein endothelial cell assays. Endothelial tube formation was assessed using HUVECs cultured on extracellular matrix. Full-growth medium was used to stimulate tube formation. IRO was added to the growth medium and tube formation was allowed to proceed for 18 h. Tube length was measured using Image Pro Plus software. IRO inhibited endothelial tube formation with an  $\text{IC}_{50}$  of 6.5  $\mu\text{mol/L}$  (Fig. 5A).

HUVEC proliferation was assessed using the [ $^3\text{H}$ ]thymidine incorporation assay. Endothelial cells were seeded into a 96-well plate, treated with different concentrations of IRO, and [ $^3\text{H}$ ]thymidine incorporation was determined. IRO inhibited endothelial cell proliferation with an  $\text{IC}_{50}$  of 0.36  $\mu\text{mol/L}$  (Fig. 5B). Proliferation was inhibited at a >20-fold lower concentration than that needed to produce cytotoxicity ( $\text{IC}_{50}$ , 8.7  $\mu\text{mol/L}$ ), estimated by reduced cellular ATP levels (Fig. 5C).

Finally, endothelial cell migration was assessed using a transwell migration assay (BD Biosciences). HUVECs were serum starved for 4 h then seeded into the top wells of migration chambers in endothelial basal medium (without growth factors). Complete medium containing growth factors was placed in the bottom well as a chemoattractant. Migration was allowed to proceed for 22 h, at which point migrated cells were fixed, stained, and quantified. IRO did not significantly affect endothelial cell migration (Fig. 5D). Collectively, the data in Fig. 5 show that IRO inhibits two major components of the angiogenic process, endothelial tube formation and cell proliferation, but does not significantly affect endothelial cell migration.

## Discussion

We have used transgenic zebrafish to create the first automated, quantitative assay capable of identifying compounds with antiangiogenic activity in a whole organism. The benefits of using live animals for phenotypic screening include the absence of time-consuming manual fixation steps. Moreover, screening in zebrafish can be performed more rapidly on a higher number of animals using much less compound than other animal models. Screening the LOPAC1280 library identified two known antiangiogenic compounds as hits, thus validating the use of the assay for antiangiogenic drug discovery. The two known antiangiogenic compounds, SU4312 and AG1478, had not been previously shown to have antiangiogenic activity in zebrafish. IRO, a novel antiangiogenic compound, was also identified.

IRO is a cell-permeable derivative of indirubin, the active component of Danggui Longhui Wan, a mixture of plants used in traditional Chinese medicine for the treatment of chronic diseases, particularly chronic myelocytic leukemia (CML). IRO and other indirubin derivatives were shown to inhibit cyclin dependent kinases (CDK; ref. 13). More recently, IRO has been shown to inhibit GSK3 $\beta$  (14), AMP-activated protein kinase, Lck, serum glucocorticoid-inducible kinase (15), and c-Jun-NH $_2$ -kinase (16) with similar potencies to its activity on CDKs. Therefore, the antiangiogenic activity of IRO may be multimodal. Interestingly, IRO was also shown to inhibit fibroblast growth factor receptor 1, which may play a role in its antiangiogenic activity (17). This work shows that IRO may have use as a therapeutic for solid tumors that rely on angiogenesis for growth, in addition to its use against CML.

We showed that IRO inhibits endothelial cell proliferation and tube formation in HUVEC assays. Importantly, the relatively low level of IRO-induced endothelial cytotoxicity shows that its

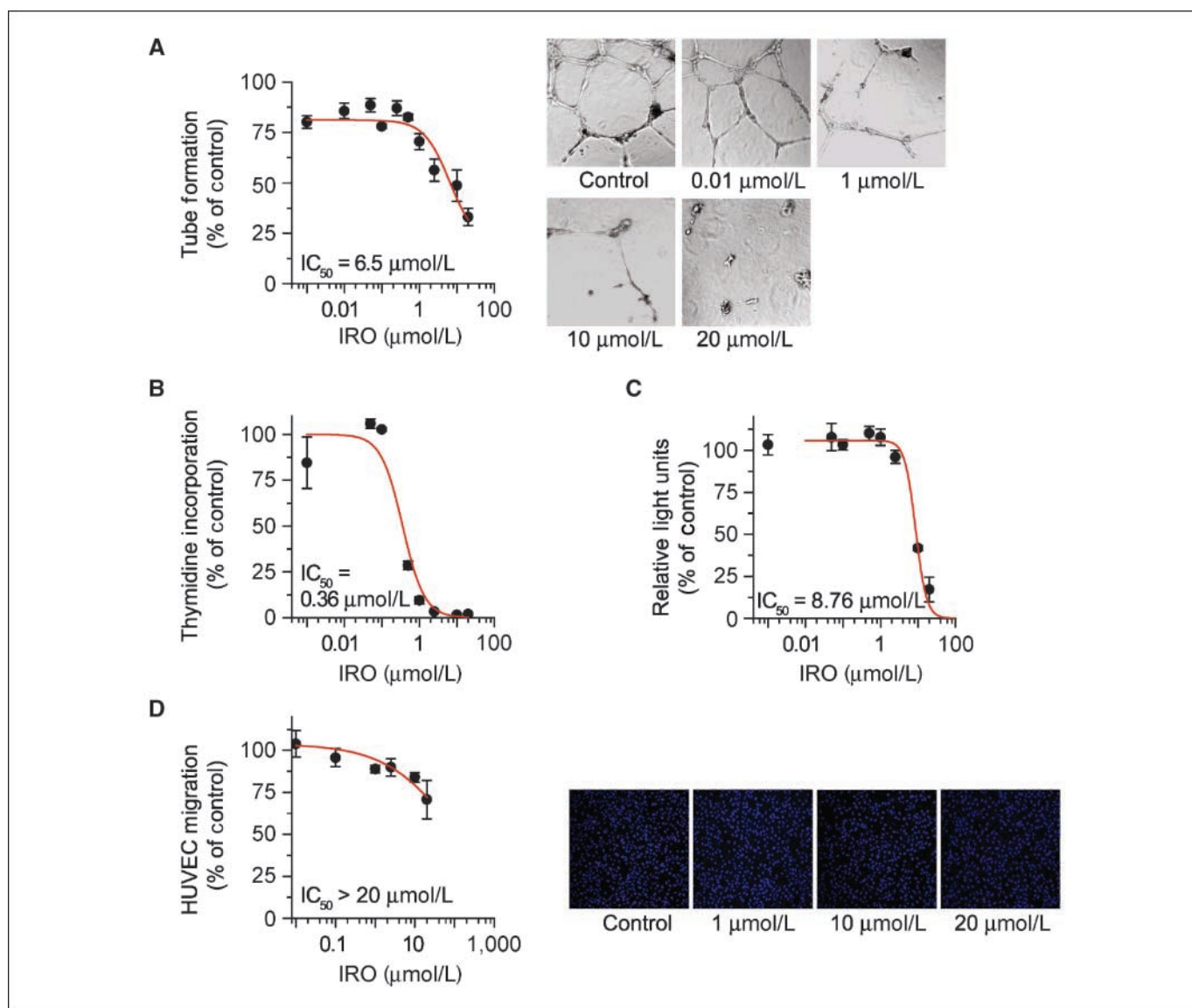


**Figure 5.** IRO inhibits *in vitro* angiogenesis. **A**, to test the effects of IRO on endothelial cell tube formation, HUVECs were plated in a 96-well plate on extracellular matrix and treated with IRO at the indicated concentrations. IRO dose-dependently inhibited tube formation. **B**, to determine the effects of IRO on endothelial cell proliferation, [<sup>3</sup>H]thymidine incorporation into cultured HUVECs treated with IRO at the indicated concentrations was assessed. IRO inhibited HUVEC proliferation in a dose-dependent manner. **C**, to test the effects of IRO on cell viability, cellular ATP levels were determined using the CellTiter-Glo Assay. **D**, to test the effects of IRO on endothelial cell migration, a transwell migration assay was performed. IRO does not significantly affect endothelial cell migration at any dose tested. Points, mean of three independent experiments; bars, SE.

antiproliferative activity is not due to broad cytotoxic effects. This is consistent with the zebrafish data, which show no observable toxicity of IRO on embryos treated with antiangiogenic doses of IRO and no effect of IRO on preexisting vasculature. This marks the first report to date of a novel antiangiogenic compound identified using zebrafish and confirmed in human cell-based assays.

The zebrafish angiogenesis assay is clearly capable of identifying known antiangiogenic compounds and useful for discovering novel antiangiogenic compounds. Despite this, five known antiangiogenic compounds in the LOPAC1280 library were not identified as hits. Two of these, SU5416 and 2-methoxyestradiol, were toxic at the screening dose but were antiangiogenic at lower, nontoxic doses. To circumvent this issue in future applications, lower compound doses can be tested to find only the most potent compounds, while avoiding toxicity. Alternatively, higher screening doses can be used

to enrich for antiangiogenic compound identification, and the activity of toxic compounds can be resolved by secondary screening at lower concentrations. Three other antiangiogenic compounds with low log *P* values, DFMO hydrochloride, minocycline hydrochloride, and thalidomide, were also not identified. Compounds with log *P* values less than 1 are typically not well-absorbed by zebrafish at commonly used screening concentrations. This is a limitation of the assay, but low log *P* compounds in a library can be identified before screening and tested by treating zebrafish embryos at high concentrations of these compounds, or by injecting these compounds into embryos. For high-throughput applications, however, low log *P* antiangiogenic compounds will likely be accepted as false negatives.

The transgenic zebrafish assay described provides a whole organism system for rapid screening of compound libraries. It

combines the physiologic complexity of an *in vivo* vertebrate model with the speed of high-throughput screening. As such, the assay may be used as a physiologically relevant primary screen, or as a bridge between biochemical or cell-based screening assays and expensive, labor-intensive mammalian systems. Compounds found to be active in primary screens can be rapidly tested in zebrafish to prioritize compounds for preclinical drug development, thus providing a valuable and efficient tool for drug discovery.

## Acknowledgments

Received 8/16/2007; revised 9/23/2007; accepted 10/3/2007.

**Grant support:** NIH grants U54 HG003918 (R. Dingledine) and R43CA117000 (E.M. Sandberg).

The costs of publication of this article were defrayed in part by the payment of page charges. This article must therefore be hereby marked *advertisement* in accordance with 18 U.S.C. Section 1734 solely to indicate this fact.

We thank Dr. Yuhong Du for help with the early stages of the study and Brian Revennaugh for data management; Drs. Zhican Qu and Anshu Roy from Southern Research Institute for performing endothelial cell-based assays; and Dr. Peter Eimon for critically reviewing the manuscript.

## References

1. Auerbach R, Lewis R, Shinnars B, Kubai L, Akhtar N. Angiogenesis assays: a critical overview. *Cancer Metastasis Rev* 2000;49:32–40.
2. Isogai S, Horiguchi M, Weinstein BM. The vascular anatomy of the developing zebrafish: an atlas of embryonic and early larval development. *Dev Biol* 2001;230:278–301.
3. Liang D, Chang JR, Chin AJ, et al. The role of vascular endothelial growth factor (VEGF) in vasculogenesis, angiogenesis, and hematopoiesis in zebrafish development. *Mech Dev* 2001;108:29–43.
4. Lyons MS, Bell B, Stainier DY, Peters KG. Isolation of the zebrafish homologues for the tie-1 and tie-2 endothelium-specific receptor tyrosine kinases. *Dev Dyn* 1998;212:133–40.
5. Chan J, Bayliss PE, Wood JM, Roberts TM. Dissection of angiogenic signaling in zebrafish using a chemical genetic approach. *Cancer Cell* 2002;1:257–67.
6. Cross LM, Cook MA, Lin S, Chen JN, Rubinstein AL. Rapid analysis of angiogenic drugs in a live fluorescent zebrafish assay. *Arterioscler Thromb Vasc Biol* 2003;23:911–2.
7. Seng WL, Eng K, Lee J, McGrath P. Use of a monoclonal antibody specific for activated endothelial cells to quantitate angiogenesis *in vivo* in zebrafish after drug treatment. *Angiogenesis* 2004;7:243–53.
8. McKinley ET, Baranowski TC, Blavo DO, et al. Neuroprotection of MPTP-induced toxicity in zebrafish dopaminergic neurons. *Brain Res Mol Brain Res* 2005;141:128–37.
9. Zhang JH, Chung TD, Oldenburg KR. A simple statistical parameter for use in evaluation and validation of high throughput screening assays. *J Biomol Screen* 1999;4:67–73.
10. Schultheiss C, Blechert B, Gaertner FC, et al. *In vivo* characterization of endothelial cell activation in a transgenic mouse model of Alzheimer's disease. *Angiogenesis* 2006;9:59–65.
11. Vinals F, Pouysseque J. Transforming growth factor  $\beta$ 1 (TGF- $\beta$ 1) promotes endothelial cell survival during *in vitro* angiogenic via an autocrine mechanism implicating TGF- $\alpha$  signaling. *Mol Cell Biol* 2001;21:7218–30.
12. Milan DJ, Peterson TA, Ruskin JN, Peterson RT, MacRae CA. Drugs that induce repolarization abnormalities cause bradycardia in zebrafish. *Circulation* 2003;107:1355–8.
13. Hoessel R, Leclerc S, Endicott JA, et al. Indirubin, the active constituent of a Chinese antileukaemia medicine, inhibits cyclin-dependent kinases. *Nat Cell Biol* 1999;1:60–7.
14. Leclerc S, Garnier M, Hoessel R, et al. Indirubins inhibit glycogen synthase kinase-3  $\beta$  and CDK5/p25, two protein kinases involved in abnormal tau phosphorylation in Alzheimer's disease. A property common to most cyclin-dependent kinase inhibitors? *J Biol Chem* 2001;276:251–60.
15. Bain J, McLauchlan H, Elliott M, Cohen P. The specificities of protein kinase inhibitors: an update. *Biochem J* 2003;371:199–204.
16. Xie Y, Liu Y, Ma C, et al. Indirubin-3'-oxime inhibits c-Jun NH2-terminal kinase: anti-apoptotic effect in cerebellar granule neurons. *Neurosci Lett* 2004;367:355–9.
17. Zhen Y, Sorenson V, Jin Y, Suo Z, Wiedlocha A. Indirubin-3'-monoxime inhibits autophosphorylation of FGFR1 and stimulates ERK1/2 activity via p38 MAPK. *Oncogene* 2007;26:6372–85. Epub 2007 May 28.